Interaction of surfactant coated PLGA nanoparticles with in vitro human brain-like endothelial cells

Elisa L.J. Moya, Sonia Lombardo, Elodie Vandenhaute, Marc Schneider, Caroline Mysiorek, Akif Türeli, Takashi Kanda, Fumitaka Shimizu, Yasuteru Sano, Nathalie Maubon, et al.

International Journal of Pharmaceutics 621 (2022) 121780

Contents lists available at ScienceDirect

International Journal of Pharmaceutics

journal homepage: www.elsevier.com/locate/ijpharm

Interaction of surfactant coated PLGA nanoparticles with in vitro human brain-like endothelial cells

Elisa L.J. Moya [a,1], Sonia M. Lombardo [b,c,1], Elodie Vandenhaute [d], Marc Schneider [c], Caroline Mysiorek [a], Akif E. Türeli [b], Takashi Kanda [e], Fumitaka Shimizu [e], Yasuteru Sano [e], Nathalie Maubon [d], Fabien Gosselet [a], Nazende Günday-Türeli [b], Marie-Pierre Dehouck [a,*]

[a] Laboratoire de la Barrière Hémato-Encéphalique (LBHE), University of Artois, UR 2465, F-62300 Lens, France
[b] MyBiotech GmbH, Industrie Str. 1B, 66802 Überherrn, Germany
[c] Department of Pharmacy, Biopharmaceutics and Pharmaceutical Technology, Saarland University, Campus C4 1, 66123 Saarbrücken, Germany
[d] HCS Pharma, F-59120 Loos, France
[e] Department of Neurology and Clinical Neuroscience, Yamaguchi University Graduate School of Medicine, Ube, Japan

ARTICLE INFO

Keywords:
Blood-Brain Barrier (BBB)
Nanocarriers
BBB in vitro models
Poly(lactide-co-glycolide) nanoparticles
Polysorbate 80
Poloxamer 188

ABSTRACT

Treatment for CNS related diseases are limited by the difficulty of the drugs to cross the blood–brain barrier (BBB). The functionalization of polymeric nanoparticles (NPs) coated with the surfactants polysorbate 80 (PS80) and poloxamer 188 (P188), have shown promising results as drugs carriers are able to cross the BBB on animal models. In this study, poly(lactide-co-glycolide) (PLGA) NPs coated with PS80 and P188, labelled with a fluorescent dye were tested on human pre-clinical in vitro model to evaluate and compare their uptake profiles, mechanisms of transport and crossing over human brain-like endothelial cells (BLECs) mimicking the human BBB. In addition, these NPs were produced using a method facilitating their reproducible production at high scale, the MicroJet reactor® technology. Results showed that both formulations were biocompatible and able to be internalized within the BLECs in different uptake profiles depending on their coating: P188 NP showed higher internalization capacity than PS80 NP. Both NPs uptakes were ATP-dependent, following more than one endocytosis pathway with colocalization in the early endosomes, ending with a NPs release in the brain compartment. Thus, both surfactant-coated PLGA NPs are interesting formulations for delivery to the brain through the BBB, presenting different uptake profiles.

1. Introduction

Drug delivery to the brain remains one of the most challenging routes. Indeed, the brain is protected by a barrier made by the tightly-joined endothelial cells of the cerebral microvessels: the blood–brain barrier (BBB) (Abbott et al., 2010). This selective barrier has a physiological goal to protect the brain from neurotoxic compounds and to maintain the brain homeostasis (Hawkins and Davis, 2005). Thus, the BBB highly restrains the access to the brain of a large variety of molecules, including most active pharmaceutical ingredients (API). The difficulty of delivering conventional formulations to the brain is one of the main explanations why so many central nervous system (CNS) diseases still have major medical needs. Indeed, CNS related diseases are positioned among the leading causes of death worldwide, and thus a huge burden for society (World Health Organization, 2021). Furthermore, with the rise of global life expectancy, this burden will only grow heavier in the coming years.

To solve this delivery issue, innovative drug delivery systems, including polymeric nanoparticles, have been developed to deliver API across the BBB. Different physiological pathways through the BBB can be used to reach the brain: the paracellular pathway, passive transmembrane diffusion, carrier-mediated transport, receptor-mediated transport (RMT) or adsorptive-mediated transport (AMT) (Abbott et al., 2006). Among them, RMT and AMT have been extensively targeted by nanocarrier systems to cross the BBB, by modifying the surface properties of nanocarriers with ligands or surfactants (Lombardo et al., 2020). Surfactants are an interesting approach to increase the BBB crossing ability of polymeric nanoparticles. In fact, coated poly(butyl

* Corresponding author.
E-mail address: mpierre.dehouck@univ-artois.fr (M.-P. Dehouck).
[1] Equal contributor.

https://doi.org/10.1016/j.ijpharm.2022.121780
Received 15 January 2022; Received in revised form 11 April 2022; Accepted 25 April 2022
Available online 3 May 2022

cyanoacrylate) (PBCA) (Ambruosi et al., 2006), poly(lactic acid) (PLA) (Ren et al., 2009), or poly(lactic-co-glycolic acid) (PLGA) nanoparticles (Gelperina et al., 2010) with polysorbate 80 (PS80) or poloxamer 188 (P188) allow the particles to cross the BBB by RMT. Indeed, PS80 and P188, both compendial surfactants used in a vast amount of drug products, can interact with apolipoproteins A-I, B and E in the blood, increasing the adsorption of these proteins on the surface of the particles. Thus, the particles might then be recognized by the LDL receptor (LDL-R), low-density lipoprotein receptor-related proteins (LRP1, LRP2, LRP8) and the scavenger receptors on the BBB (Kreuter et al., 2002; Petri et al., 2007). However, the studies focusing on the pathway taken by surfactant-coated nanoparticles through the brain endothelial cells have only been performed on PBCA nanoparticles, to the best of our knowledge. Surfactant-coated PLGA nanoparticles have been also widely used in vitro and in vivo to deliver various compounds to the brain, with variable success depending on their cargo and the surfactant used (Lombardo et al., 2020). Indeed, in a study by Gelperina et al, PS80 and P188-coated PLGA nanoparticles have been used in vivo for the delivery of doxorubicin and loperamide. In both-case, P188-coated nanoparticles showed the highest efficacy (Gelperina et al., 2010). However, in another in vivo study by Tahara et al, PS80-coated PLGA nanoparticles loaded with 6-coumarin had a higher BBB crossing than P188-coated nanoparticles (Tahara et al., 2011). PS80-coated PLGA nanoparticles were also reported to have superior BBB penetration in vitro and in vivo compared to uncoated nanoparticles (Chaturvedi et al., 2014) but some other studies reported a superior accumulation of PS80-coated PLGA nanoparticles in the lung rather than in the brain (Miyazawa et al., 2015). Thus, a better understanding on the mechanisms of crossing and uptake of surfactant-coated PLGA nanoparticles might help explain the discrepancies observed in efficacy of these formulations in vitro and in vivo, rather than just assuming that PLGA nanoparticles have the same BBB crossing mechanisms as PBCA nanoparticles. Furthermore, those in vivo experiments performed on rodents, could present BBB interspecies differences from the human BBB, which might be one of the reasons why some promising formulations from in vivo pre-clinical trials fail once in clinical trials. Therefore, gaining knowledge on preclinical human models might be relevant for early-stage drug discovery to prevent some of these failures. Polysorbate 80 and poloxamer 188 have already been approved by the FDA for intravenous applications (U.S Food and Drug Administration, 2022). In addition, PLGA and PLA are biocompatible and biodegradable polymers, already approved by the FDA for the parenteral route too (Makadia and Siegel, 2011; Lee et al., 2016). However, functionalizing the polymers with ligands, as it is done in many carrier systems for brain delivery, means physically modifying the polymer and changing its proven quality and safety aspects that led to its approval. This would mean that the modified polymer must be intensively studied for these aspects and undergo a new regulatory approval process. Thus, by simply coating the polymer with surfactants instead, without any covalent modifications, the studies needed to bring the nanoparticles to the market can be reduced when compared to functionalized particles.

Another bottleneck for the access to the market of nanoparticles is their production method. Nanoparticles must be produced at large scale homogeneously in a reproducible manner for each batch. Most nanoparticle preparation techniques after scale-up produce poorly reproducible nanoparticles with a high polydispersity index (PDI), due to difference in batch composition between the beginning and the end of the production, leading to the production of nanoparticles with a wide size range. To tackle this issue, continuous production methods have been developed such as double emulsification spray-drying method (Schiller et al., 2020), emulsion-solvent diffusion method by focused ultrasound (Schiller et al., 2015), microfluidic techniques (Valencia et al., 2012; Makgwane and Ray, 2014) or the MicroJet reactor® (MJR) technology.

The MJR technology, a continuous impinging jet method in a confined chamber, was used to prepare our nanoparticles. Indeed, this manufacturing technique allows the production of highly reproducible nanoparticles at large scale by fully controlling the parameters of the process (Günday Türeli et al., 2016). The solvent solution and non-solvent solution are pumped on opposite sides of a confined reactor. The two jets meet in the reactor and mix immediately, forming nanoparticles by nanoprecipitation. Nitrogen gas can also be added by a third entry to help the ejection of the nanoparticles out of the reactor. The nanoparticles exit the reactor by a fourth opening, at the bottom (Fig. 1). The main advantage of this method is that the mixing properties stay the same for the whole duration of the process, as opposed to benchtop nanoprecipitation where differences in mixing can occur due to the difference of composition of the mixture between the beginning of the solvent addition and the end. Thus, more reproducible nanoparticles with low PDI can be obtained with the MJR at large scale than with classical benchtop production. By adjusting the process parameters such as diameter of the reactor, the flow rates of the solutions, the temperature and if necessary, the gas pressure, the mixing of the two solutions can be optimized to form nanoparticles of small size and low PDI (Günday Türeli et al., 2016).

Hence, the aim of this study was to evaluate and compare the cellular interaction and pathway taken of PLGA nanoparticles coated with PS80 or P188, labelled with the fluorescent probe Lumogen F Red 305®, prepared using the MJR technology through the BBB with a well-established human pre-clinical in vitro BBB model (Cecchelli et al., 2014; Moya et al., 2021). This model was formed by CD34+ stem cell-derived endothelial cells (CD34+-ECs) seeded in the upper compartment of an insert, representing the luminal compartment (blood side), in a non-contact coculture with brain pericytes seeded in the bottom wells, representing the brain compartment. In these culture conditions, the CD34+-ECs acquired BBB endothelial cells phenotype properties and were named brain-like endothelial cells (BLECs). The models were adapted for this specific NPs research study using human serum as a supplement of the cell medium. The NPs toxicity, uptake, mechanisms of transport and crossing through the BLECs were investigated and compared to each other.

2. Material and methods

2.1. NP production and characterization

The nanoparticles were produced by nanoprecipitation using the continuous MicroJet reactor technology. The nanoparticle composition and their production process were optimized to obtain small nanoparticles below 100 nm. The solvent solution was composed of 0.1% (w/v) PLGA Resomer® RG 502H 50:50 (Evonik, Essen, Germany) and 2.8×10^{-4} % (w/v) Lumogen F Red 305® (BASF, Ludwigshafen, Germany) in acetone. The non-solvent solution was prepared by dissolving either

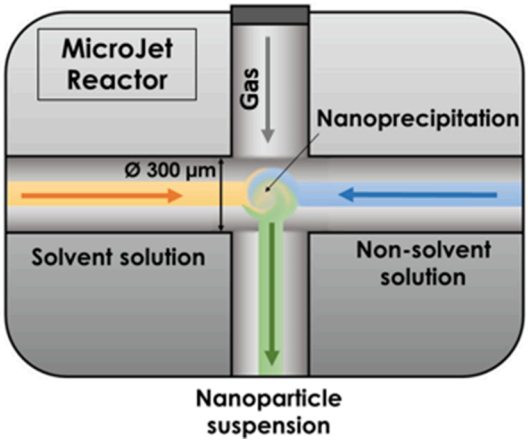

Fig. 1. Nanoprecipitation in MicroJet reactor.

polysorbate 80 (Tween® 80, ref. 8.17061, Merck, Darmstadt, Germany) or poloxamer 188 (Kolliphor® P188, ref. 15759, Sigma-Aldrich, Saint-Louis, USA) at 1% (w/v) in distilled water. A 300 μm reactor was used. The particles were prepared in a 25 °C water bath. The solvent solution was pumped at 25 ml/min in the reactor while the non-solvent solution was pumped at 50 ml/min, thus preparing the nanoparticles with a solvent:non-solvent ratio of 1:2 (v/v). Acetone was evaporated by stirring the nanoparticles under the hood, protected from light. The nanoparticles were then purified using Tangential Flow Filtration (TFF) to remove excess surfactant and free dye using a Spectrum® 100 kD 20 cm^2 MicroKros hollow fiber membrane (ref. C02-E100-05-N, Repligen, Waltham, USA). The particles were purified at 15 psi with 6 volumes of water for P188 NP, and with 12 volumes for PS80 NP, as a higher amount of unencapsulated dye needed to be washed out. The nanoparticles mean hydrodynamic size, size distribution (PDI), and zeta potential were measured by Dynamic Light Scattering (DLS) using a Zetasizer® NanoZS 90 (Malvern Instruments, Malvern, UK). After purification, the nanoparticles were diluted 10-fold in water and measured once at 25 °C, with 12 runs each. After production, a known volume of nanoparticles was dried using a freeze dryer and the weight of the nanoparticles after drying was measured, allowing us to calculate their mass concentration. The nanoparticles were then diluted accordingly in cell medium to obtain the wanted concentrations for the study.

2.2. Human in vitro BBB coculture models

Human BBB in vitro models were produced using human brain-like endothelial cells (BLECs) according to the protocol developed by Cecchelli et al. (2014). First, CD34+ hematopoietic stem cells isolated from human umbilical cord blood using the method described by Pedroso et al. (2011) were differentiated in endothelial cells. Then, BLECs were obtained after non-contact coculture with brain pericytes (PCs) (Vandenhaute et al., 2011; Shimizu et al., 2011), using Transwell (TW) systems.

Different TW system formats were used to develop the human BBB in vitro models in this study. A miniaturized and automated model in 96 multiwell system (Moya et al., 2021) was used for the NPs screening evaluation at different concentrations and time-points. This model was developed as a replicate from the original well-established and patented model from Cecchelli et al. (2014). Moreover, for the NPs uptake and transport experiments, the original model in 12 Transwell (TW) format in a syngeneic form was used. The miniaturized system was developed in 96 multiwell insert format (Falcon, Corning Life science, Massachusetts, USA. Plates 1 μm Polyethylene Terephthalate (PET), ref. 351131; 0.0804 cm^2 cell growth surface area) as a coculture with bovine pericytes (Vandenhaute et al., 2011) by automated seeding of 15,000 PCs per well, and 18,000 ECs per filter, using a Multiflo robot (BioTek Instruments, Winooski, VT, USA), while the syngeneic original model was developed in 12 TW plates (Corning, New York, USA. Plates 0.4 and 3 μm Polycarbonate (PC) filters; ref. 3401 and ref. 3402 respectively; 1.12 cm^2 cell growth surface area) as a coculture with human pericytes provided by Professor Takashi Kanda's group (Department of Neurology and Clinical Neuroscience, Yamaguchi University Graduate School of Medicine, Ube, Japan) (Shimizu et al., 2011). The cells were seeded by hand 50,000 PCs per well, and 80,000 ECs per filter.

To produce the human coculture BBB models, brain PCs were seeded on bottom well plates coated with pig gelatin (2 mg/L; Sciencell, Carlsbad, USA) for bovine PCs, and with rat tail type I collagen for human PCs (10 μg/cm^2; Corning, New York, USA) in ECM(5%FCS), which consists of basal endothelial cell medium (ECM; Sciencell, Carlsbad, USA) supplemented with 5% FCS, 1% endothelial cell growth supplement (Sciencell, Carlsbad, CA, USA) and 0.5% gentamicin (Biochrom AG, Berlin, Germany). The cells were incubated during 3 h at 37 °C. Next, CD34+-derived ECs were seeded on Transwell inserts coated with Matrigel™ diluted by 1/48 (v/v) (BD Biosciences, San Jose, CA, USA) and immediately cocultured with brain PCs seeded on the bottom wells of the plates. However, to generate the coculture model in 3 μm porosity filter, the 80,000 CD34+-derived ECs were seeded on Transwell inserts one week before their coculture with the PCs (Vandenhaute et al., 2016). The medium was renewed every 2 days. On day 5 of coculture, 24 h before incubation with the nanoparticles (NPs), ECM supplemented with 5% FCS (ECM(5%FCS)) was substituted by 5% human serum (ECM(5%HS)) obtained from "l'Etablissement Français du Sang" (EFS), following an agreement with the Artois University. After 6 days of coculture with brain pericytes, the BBB endothelial cells acquired the BBB phenotype (named brain-like endothelial cells (BLECs) at that stage) and were used for the following experiments.

2.3. BBB integrity evaluation after nanoparticles treatment

The BLECs physical integrity was evaluated by measuring the diffusion of the integrity marker sodium fluorescein (NaFlu; Sigma Aldrich, Darmstadt, Germany), a small hydrophilic molecule which poorly crosses the intact BBB. Human BBB miniaturized models were developed for the evaluation of the impact of the nanoparticles, at different concentrations and time-points, on the BBB integrity. The NPs were diluted in ECM(5%HS) to achieve a concentration of 5, 10, 25, 50, and 100 μg/ml NPs. The NPs were added in the luminal compartment of the BLECs inserts and incubated during 3, 6, and 24 h at 37 °C. BLECs incubated in ECM(5%HS) without NPs for 24 h were used as negative control. As positive control of BBB disruption, a neurotoxic compound, Rotenone, was incubated also during 24 h (Moya et al., 2021; Ravenstijn et al., 2008). At the end of the incubation time, the BLECs physical integrity was evaluated by measuring NaFlu diffusion. To do so, the BLECs inserts were transferred into new 96 TW systems (Falcon HTS 96 square well; ref. 353925; Corning Life science, Massachusetts, USA) containing 300 μl of Ringer-HEPES (RH) solution (150 mM NaCl, 5.2 mM KCl, 2.2 mM CaCl2, 0.2 mM MgCl2·6H2O, 6 mM NaHCO3, 5 mM HEPES, 2.8 mM glucose; pH 7.4) per well which constituted the abluminal compartment. The cell culture medium from the BLECs inserts containing NPs dilution was removed, and 70 μl of RH solution containing 1 μM NaFlu (the integrity marker) were added in the upper (luminal) compartment. RH was used to avoid any interference of the cell phenol red media with NaFlu. The cells were incubated at 37 °C for 1 h. Next, aliquots from the lower and upper compartments were collected, as well as from the stock solution at time zero. Their fluorescence at excitation/emission wavelength 490/525 nm was measured using a fluorimeter (Synergy H1; BioTek, Winooski, VT, USA) in a 96-well plate. The endothelial permeability coefficient (Pe) of NaFlu was calculated in cm/min. The clearance principle was used to obtain a concentration-independent index of transport. Briefly, the mean volume cleared was plotted against time, and the slope was estimated by linear regression. The permeability values of the inserts (PSf, for inserts with a Matrigel coating only) and the inserts plus BLECs (PSt, for inserts with matrigel coating and cells) were taken into consideration by applying Eq. (1):

$$1/PSe = 1/PSt - 1/PSf \quad (1)$$

To obtain the endothelial permeability coefficient (Pe, in cm/min), the permeability value (PSe) corresponding to the endothelium alone was then divided by the insert porous membrane surface area (S) (S = 0.0804 cm^2 cell growth surface area for 96 TW system, or S = 1.12 cm^2, for 12 TW plates) (Eq. (2)).

$$Pe = PSe/S \quad (2)$$

2.4. Cell visualization by confocal microscopy

2.4.1. Cells fixation

BLECs were fixed on their inserts and PCs were fixed on the bottom wells using paraformaldehyde 4% (PFA, ref. HT5014; Sigma-Aldrich, Darmstadt, Germany) for 10 min. Then, the cells were washed 3 times

during 5 min with calcium and magnesium-free phosphate buffered saline (PBS-CMF).

2.4.2. Immunocytochemistry

After cell fixation, permeabilization was done with Triton 0.1% (w/v) (Sigma-Aldrich, Darmstadt, Germany) and the cells were again washed 3 times during 5 min with PBS-CMF. Cells were incubated with SEA BLOCK blocking buffer (ref. 37527; Thermo Fisher Scientific; Massachusetts, USA) for 30 min. BLECs were incubated away from light for 1 h at room temperature with primary antibodies against zonula occludens-1 (ZO-1) (ref. 617300; Invitrogen; Thermo Fisher Scientific; Massachusetts, USA), diluted by 200 in PBS-CMF supplemented with 2% (v/v) normal goat serum (NGS). After three washing steps with 2%NGS-PBS-CMF, BLECs were incubated with secondary antibodies for 30 min at room temperature using goat anti-rabbit Alexa Fluor 488 (Invitrogen, Massachusetts, USA; dilution: 1/500 in 2%NGS-PBS-CMF). Nuclei were stained using Hoechst reagent (ref. B2883; Sigma-Aldrich, Darmstadt, Germany) diluted 1,000 times in the same secondary antibody solution. Finally, the cells were washed 3 times during 5 min with PBS-CMF. Filters with BLECs for miniaturized model were directly placed in the microscope, while 12 TW inserts were cut and mounted on a glass slide under a coverslip. Stained preparations were observed with an ImageXpress Micro Confocal High-Content Imaging System (Molecular devices, San Jose, CA, USA), using blue DAPI filter (excitation/emission wavelength 358/461 nm) for nuclei, green Fluorescein isothiocyanate (FITC) filter (excitation/emission wavelength 480/530 nm) for ZO-1. Images were processed in MetaXpress software version 6.5.2 (2018, Molecular Devices, LLC, San Jose, CA, USA).

2.4.3. Nanoparticles visualization

Human BBB miniaturized model was used for the NPs visualization over different concentrations and incubation time-points. Thus, the NPs were diluted in ECM(5%HS) at concentrations of 5, 10, 25, 50 and 100 μg/ml of NPs. The NPs were added in the luminal compartment of the BLECs inserts and incubated during 3, 6, and 24 h at 37 °C. At the end of the nanoparticles' incubation time, BLECs inserts were rinsed 5 times with cold RH, and fixed as described above. Nuclei were stained using Hoechst reagent diluted by 1,000 in 2%NGS-PBS-CMF for 15 min at room temperature, away from light. Inserts with BLECs from the miniaturized 96 TW systems were placed directly over the microscope, visualizing the BLECs from the abluminal face. NPs were observed using a red Texas Red filter (excitation/emission wavelength 580/620 nm); and nuclei using a blue DAPI filter (excitation/emission wavelength 358/461 nm) using ImageXpress Micro Confocal High-Content Imaging System (Molecular devices, San Jose, CA, USA). Images were processed in MetaXpress software version 6.5.2 (2018, Molecular Devices, LLC, San Jose, CA, USA).

2.4.4. Early endosomes staining for NPs colocalization study

For NPs colocalization study, 12 TW models (0.4 μm filters) were used. After the end of the 30 min incubation period, BLECs inserts were rinsed 5 times with cold RH, and cells were fixed as described above. Primary antibodies against early endosome vesicles (EEA-1) (ref. MA5-14794; Invitrogen, Massachusetts, USA) diluted by 100 in 2%NGS-PBS-CMF were incubated for 2 h at room temperature, away from light. After three washing steps in 2%NGS-PBS-CMF, the samples were incubated with secondary antibodies for 30 min at room temperature (goat anti-rabbit Alexa Fluor 488, Invitrogen, Massachusetts, USA; dilution: 1/500 in 2%NGS-PBS-CMF). Finally, the cells were washed again three times for 5 min with PBS-CMF. Filters were cut and mounted on a glass slide with a drop of DAPI mounting medium (ref. P36962, Thermo Fisher Scientific; Massachusetts, USA) under a coverslip. BLECs were observed from the luminal face. Stained preparations were observed by confocal microscopy using a Zeiss Axio Observer LSM 710 Scanning Module coupled with ZEN 2 (blue edition) software (Zeiss, Jena, Germany). The nanoparticles were visualized with an excitation/emission wavelength 561/629 nm, detection range 603–656 nm. The EEA-1 stained with Alexa Fluor 488 was visualized with an excitation/emission wavelength 488/525 nm, detection range 496–554 nm. The nuclei stained with DAPI were visualized with an excitation/emission wavelength 561/613 nm, detection range 410–507 nm.

2.5. NPs uptake and mechanisms of internalization

2.5.1. NPs uptake studies

For NPs uptake studies, both miniaturized and 12 TW models (0.4 μm filters) were used. After incubation time was reached, in order to remove the NPs not internalized stuck on the cell surfaces, BLECs inserts were rinsed 5 times with cold RH. Then, cells were lysed using RIPA buffer (PierceTM, Thermo Scientific, Massachusetts, USA). Aliquots of 25 μl (for 96 TW systems) and 200 μl (for 12 TW model) were collected from each insert. Fluorescence analysis was done in a black color 96-well plates (ref. 137101; Thermo Scientific, Massachusetts, USA) at sensitivity 110, excitation/emission wavelength 578/613 nm, using a Synergy™ H1 fluorimeter (BioTek Instruments, Winooski, VT, USA).

2.5.2. Nps co-incubation with other molecules

Human BBB model in 12 TW plates (0.4 μm filters) were used in this experiment. To evaluate a possible receptor competition, NPs were diluted at 10 μg/ml in ECM(5 %HS) and were mixed with either Alexa Fluor 488 acetylated low density lipoproteins (acLDL) (ref. L23380; Fisher Scientific, New Hampshire, USA) or BodipyFLTM low density lipoproteins (LDL) (ref. L3483; Fisher Scientific, New Hampshire, USA), both molecules internalized by receptor mediated endocytosis (Dehouck et al., 1997), or Inulin-FITC (ref. F3272; Sigma Aldrich, Merck KGaA Darmstadt, Germany), a molecule with non-specific vesicular transport (Candela et al., 2010; Saint-Pol et al., 2013), at 15 μg/ml. Molecules with NPs mixtures were added in BLECs inserts and incubated for 1 h at 37 °C. Cells incubated with NPs only were used as uptake control. NPs cell uptake was measured as described above.

2.5.3. Cell metabolism experiments

This experiment was performed using human BBB model in 12 TW plates (0.4 μm filters). BLECs were pre-incubated at 4 °C during 90 min. NPs were diluted to 10 μg/ml in ECM(5%HS), added to the luminal compartment, and incubated for 1 h at 4 °C. NPs cell uptake was measured as described above. Inulin-FITC, used as negative control, was incubated at a concentration of 15 μg/ml, and Alexa Fluor 488 acLDL at 15 μg/ml as positive control.

2.5.4. Inhibitors of transport

Both formats, miniaturized BBB model and 12 TW models, were used for these experiments. A set of transport inhibitors were tested to assess their effects on endocytic transport (Okura et al., 2008; Georgieva et al., 2011; Morad et al., 2019). Preliminary tests of a wide concentration range of inhibitors (from Sigma Aldrich, Merck KGaA Darmstadt, Germany, except for FCCP (Carbonyl cyanide 4-(trifluoromethoxy)phenylhydrazone) purchased from Abcam, Cambridge MA, USA) were done, to assess their toxic impact on the BLECs. After optimization, BLECs were pre-incubated for 45 min at 37 °C with the following inhibitors: FCCP at 20 μM (ref. ab120081, Abcam) inhibitor of ATP dependent active transport; filipin III at 5 μg/ml (ref. F4767) and genistein at 30 μg/ml (ref. G6649), both inhibitors of caveolae endocytic routes; dynasore hydrate at 400 μM (ref. D7693) and chlorpromazine hydrochloride at 20 μg/ml (ref. 215921), both inhibitors of clathrin-mediated endocytosis; 5-(N,N-dimethyl)amiloride hydrochloride (dimethylamiloride) at 60 μM (ref. A4562) and cytochalasin D at 1 μM (ref. C8273), both inhibitors of macropinocytosis. All inhibitors were diluted in ECM(5%HS). Next, NPs were added in the luminal compartment at 10 μg/ml and incubated for 1 h. NPs cell uptake was measured as described above.

2.6. NPs crossing through BLECs

Crossing studies were performed using the 12 TW format (3 μm filters) as previously described (Vandenhaute et al., 2016). One day before the experiment, ECM(5%FCS) was substituted for ECM5 (HS) phenol red free (PRF) (ref. 1001-prf; Sciencell, Carlsbad, USA) (ECM(5%HS)-PRF), in order to facilitate NPs detection within the cell medium. Then, NPs were diluted to 10 μg/ml in ECM(5%HS)-PRF and added to the luminal compartment and incubated during 3, 6 and 24 h. At the end of the incubation times, aliquots from the luminal (L) and abluminal (A) compartments were taken, as well as samples from the initial dilution (t0). Fluorescence was measured in a black color 96-well plate (ref. 137101; Thermo Scientific, Massachusetts, USA) at sensitivity 110, excitation/emission wavelength 578/613 nm, using a Synergy™ H1 fluorimeter (BioTek Instruments, Winooski, VT, USA). The background emitted by the medium was subtracted and the percentage of crossing (Eq. (3)) and NPs recovery (Eq. (4)) were calculated using the following equations:

$$\%\ \text{Crossing} = 100 \times (\text{Quantity A (tx)} \,/\, \text{Initial Quantity (t0)}) \quad (3)$$

$$\%\ \text{Recovery} = 100 \times (\text{Quantity A (tx)} + \text{Quantity L (tx)}) \,/\, \text{Initial Quantity (t0)} \quad (4)$$

2.7. Statistical analysis

Results were expressed as mean ± standard deviation (SD). The number of replicates (n), performed through independent experiments (N), were detailed in each experiment. For analysis involving two groups, unpaired *t*-test, or one-way ANOVA, followed by Bonferroni's multiple comparison tests was used. For analysis of more than one condition in two groups, multiple *t*-test or two-way ANOVA were used. All data was analyzed by GraphPad Prism 8.1 software (GraphPad Software, San Diego, CA, USA). The threshold for statistical significance was set to p-value < 0.05.

3. Results

3.1. NPs production

PLGA NPs, coated with polysorbate 80 (PS80) or poloxamer P188 (P188), labelled with a fluorescent probe Lumogen F Red 305®, were prepared using the MJR technology. Both nanoparticle formulations had sizes close to 70 nm and negative zeta potential due to the carboxylic acid end groups of PLGA (Table 1). Even with a slightly broad distribution (PDI > 0.2), the nanoparticles produced still had mostly sizes below 150 nm. Furthermore, around 70% of the particles had size under 100 nm, which was the targeted size, as small nanoparticles under 100 nm have been reported to cross the BBB more readily (Lombardo et al., 2020).

3.2. Human BBB in vitro model development

In this study, the human BBB in vitro model used was based on well-established model using brain-like endothelial cells (BLEC) derived from hematopoietic stem cells CD34+ cocultivated with brain pericytes. This model was adapted for the NPs study by replacing fetal calf serum by human serum to be closer to human conditions.

Table 1
Nanoparticles size (N = 10) and zeta potential (N = 5).

Nanoparticles	Size (nm)		PDI		Zeta Potential (mV)	
	Mean	SD	Mean	SD	Mean	SD
PS80 NP	76.1	15.4	0.288	0.090	−39.2	1.3
P188 NP	68.9	2.9	0.230	0.032	−43.8	2.6

NPs interact not only with the cells but also with components present in the media and the serum, which adsorb on the nanoparticles to form a protein corona around them. To try to obtain a protein corona closer to the one expected to form in human blood, the fetal calf serum (FCS) classically used in the cell medium for the model development, was substituted 24 h before experiments with human serum (HS) (Fig. 2.A). Hence, after a coculture of 6 days, the BBB phenotype of the CD34+-ECs was validated by the presence of zonula occludens-1 (ZO-1) expression, a protein involved in the tight junctions and located continuously at the edge of these cells (Fig. 2.B). Moreover, the impact of the change in serum composition on the BLECs layer integrity was controlled using NaFlu, an integrity marker. No significant differences ($p = 0.8663$) were found between the model supplemented with FCS or HS. Hence, FCS could be replaced by HS without inducing disruption of BBB properties during the experimental conditions.

3.3. BBB integrity evaluation after NPs treatment

By using the BBB miniaturized system, the evaluation of NPs interaction within BLECs over concentrations and time was performed. The BBB integrity was evaluated by calculating the permeability coefficient of the integrity marker NaFlu after incubation with NPs from 5 to 100 μg/ml, for 3, 6 and 24 h. Filters without NPs treatment incubated during 24 h acted as negative control. Rotenone, a neurotoxic compound, was incubated for 24 h and used as a BBB breakdown control. Results showed no significant differences ($p > 0.05$) in the BLECs permeability to the integrity marker (Pe NaFlu) between the control (no NPs) and both NPs formulation, PS80 and P188 NP over the different concentrations and time-points studied (Fig. 3). The BBB tightness integrity was not impacted; hence NPs treatment did not show toxicity in the range of concentrations and time points tested up to 100 μg/ml and 24 h incubation.

3.4. Evaluation of PS80 and P188 coated PLGA NPs transport pathway

3.4.1. NPs internalization and visualization within BLECs

By using the automated ImageXpress Micro Confocal High-Content Imaging System, both NPs could be seen in the cell cytoplasm of BLECs at different concentrations (5–100 μg/ml) and incubation times (3, 6 and 24 h) (Fig. 4), meaning that both surfactants coated PLGA NPs could be internalized by the BLECs. From visual inspection, NPs seemed to present two different profiles. P188 NP uptake increased with incubation time and concentration, showing some fluorescence pixels saturation at the highest concentrations tested. However, PS80 NP uptake was more stable at low concentrations until 25 μg/ml, and seemed to increase at 50 μg/ml and 100 μg/ml.

3.5. NPs uptake profile

The uptake profiles of the formulations were also evaluated at low concentrations and short time, by cell lyses. BLECs were incubated with the NPs, lysed, and the fluorescence intensity of the loaded dye was quantified (Fig. 5). First, the NPs uptake was studied depending on the NPs concentration, from 5 to 25 μg/ml to avoid fluorescence saturation within the BLECs, for 90 min. The formulations again showed two different profiles (Fig. 5). After 90 min of incubation, P188 NP was uptaken in significantly higher quantities than PS80 NP by the BLECs, at 10 and 25 μg/ml (Fig. 5A). Moreover, P188 NP uptake increased with NPs concentrations and incubation time after 60 min (Fig. 5B). Meanwhile, PS80 NP uptake was not impacted by incubation time or by concentration, the uptake seemed to be already maximal at the lowest concentration and time tested, around 3%. However, P188 NPs could be uptaken more readily by the BLECs up to 30% at 25 μg/ml, after 90 min.

3.5.1. Active metabolism decrease

In a temperature dependent experiment, a significant decrease ($p <$

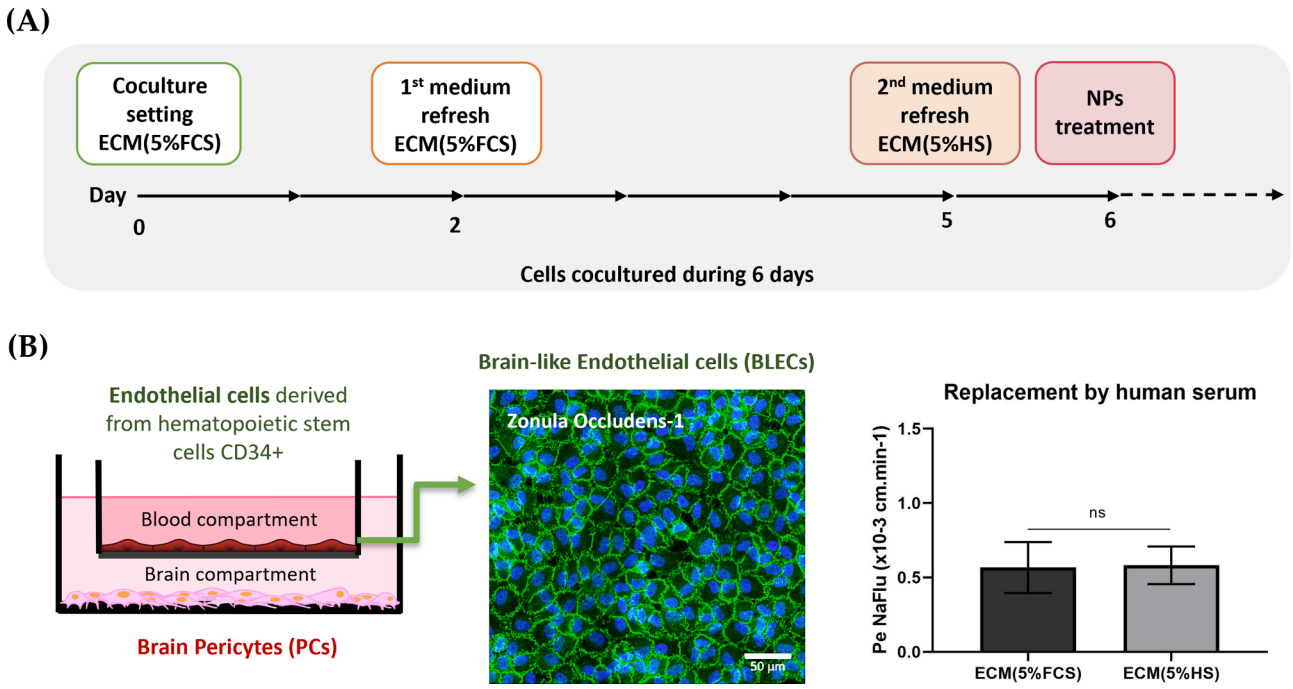

Fig. 2. Human BBB in vitro model characteristics and conformation. **A.** Schematic representation of the human in vitro BBB model cell culture protocol followed for NPs studies. Two days after cell thawing in Endothelial cell medium (ECM) supplemented with 5% FCS, brain-like endothelial cells (BLECs) were cultured on the luminal side of the insert in a non-contact coculture with brain pericytes (PCs), seeded on the plates, the abluminal side of the setup. First medium refresh was done 2 days after the coculture setting. Then, 24 h before NPs studies, a second medium refresh was done using ECM supplemented with 5% Human Serum (HS). **B.** After 6 days of coculture, BLECs were visualized by immunostaining of zonula occludens-1 (ZO-1), a protein involved in the tight junctions (scale bar = 50 µm). Endothelial permeability coefficient (Pe) to sodium fluorescein (Pe NaFlu) of the coculture model supplemented with ECM(5%FCS) as control, or with ECM(5%HS). ns = not significant. Statistical analyses of unpaired *t*-test, $p < 0.05$, $n = 6$; $N = 2$.

0.005) of 70–80% in NPs uptake could be observed when cell metabolism was decreased by incubating the cells at 4 °C (Fig. 6A). Thus, both PLGA surfactant coated NPs internalization pathways were significantly reduced. Acetylated low density lipoproteins (acLDL) uptake by receptor-mediated endocytosis (RMT) through scavenger receptors was used as a positive control. AcLDL uptake was also significantly decreased, whereas inulin uptake, a molecule with non-specific transport used as negative control, did not show any significant differences between 4 °C and 37 °C. Moreover, when an ATP synthesis inhibitor, FCCP, was added in the cell medium for both nanoparticle formulations, a significant decrease ($p < 0.0005$) of 50% in NPs uptake could also be observed (Fig. 6B). Thus, both formulation uptake mechanisms were active transport-dependent.

3.5.2. *NPs co-incubation with LDL, acLDL and inulin*

To check whether LDL or acLDL could compete with the surfactant coated PLGA NPs or promote the uptake of PLGA NPs, both formulations were co-incubated with LDL, acLDL, and inulin used as negative control. NPs uptake was measured (Fig. 6C). A significant decrease ($p = 0.000379$) in NP uptake by more than 50% for both PS80 and P188 NP was observed when co-incubated with acLDL, in addition to a slight but not significant decrease ($p = 0.0519$) when co-incubated with LDL. No significant decrease in uptake was observed when the NPs were co-incubated with inulin ($p = 0.230$). Thus, a clear specific receptor competition between acLDL and the NPs seemed to occur, in addition to a slight interference with LDL receptors.

3.5.3. *Response to metabolic inhibitors of distinct vesicular endocytosis pathways*

The NPs internalization pathways were studied by testing a range of selected inhibitors involved in different metabolic internalization routes in the BLECs. Inhibitors for caveolae (filipin III and genistein), clathrin (dynasore and chlorpromazine) and macropinocytosis (cytochalasin D, and dimethylamiloride) pathways were tested (Fig. 7A). Their non-toxic impact over the BLECs of the inhibitors was previously studied (data not shown). While a decrease of P188 NP uptake could be observed with genistein and chlorpromazine, no significant differences were found for any of the inhibitors. However, a significant decrease of the uptake could be observed for PS80 NP, with filipin III ($*p = 0.0145$) and chlorpromazine ($**p = 0.0033$), at 67% from control. Thus, the NPs seemed to internalize using both caveolae and clathrin-mediated endocytosis pathways.

3.5.4. *Colocalization with early endosomes*

To study whether NPs were internalized through a vesicular endocytosis pathway and localized within the BLECs cytoplasm, immunostaining against early endosomes vesicles (EEA-1) was performed after incubating the BLECs with P188 NP and PS80 NP independently for 30 min and 1 h. P188 and PS80 NP could be seen mostly colocalized with EEA-1 or close to each other (Fig. 7B). The presence of NPs colocated with EEA-1 indicates that the NPs followed the endocytosis metabolic process of the BLECs.

3.6. *Evaluation of P188 and PS80 NP crossing through BLECs*

NPs were incubated in the luminal compartment of BLECs at 10 µg/ml for 3, 6 and 24 h. The amount of nanoparticles in the abluminal compartment after the end of the incubation time was quantified by fluorometry and the percentage of crossing through the BBB was calculated. Both nanoformulations could be found in the abluminal compartment, showing the ability of the nanoparticles to cross through the BBB endothelium (Fig. 8A). Both formulations showed a similar transport profile at 3 and 6 h of incubation, of 1.5–2% of crossing, meaning 0.15–0.2 µg/ml NPs. However, at 24 h, PS80 nanoparticles showed a significantly higher ($*p = 0.0278$) transport percentage of 3% (0.3 µg/ml), compared to P188 NPs transport percentage which stayed

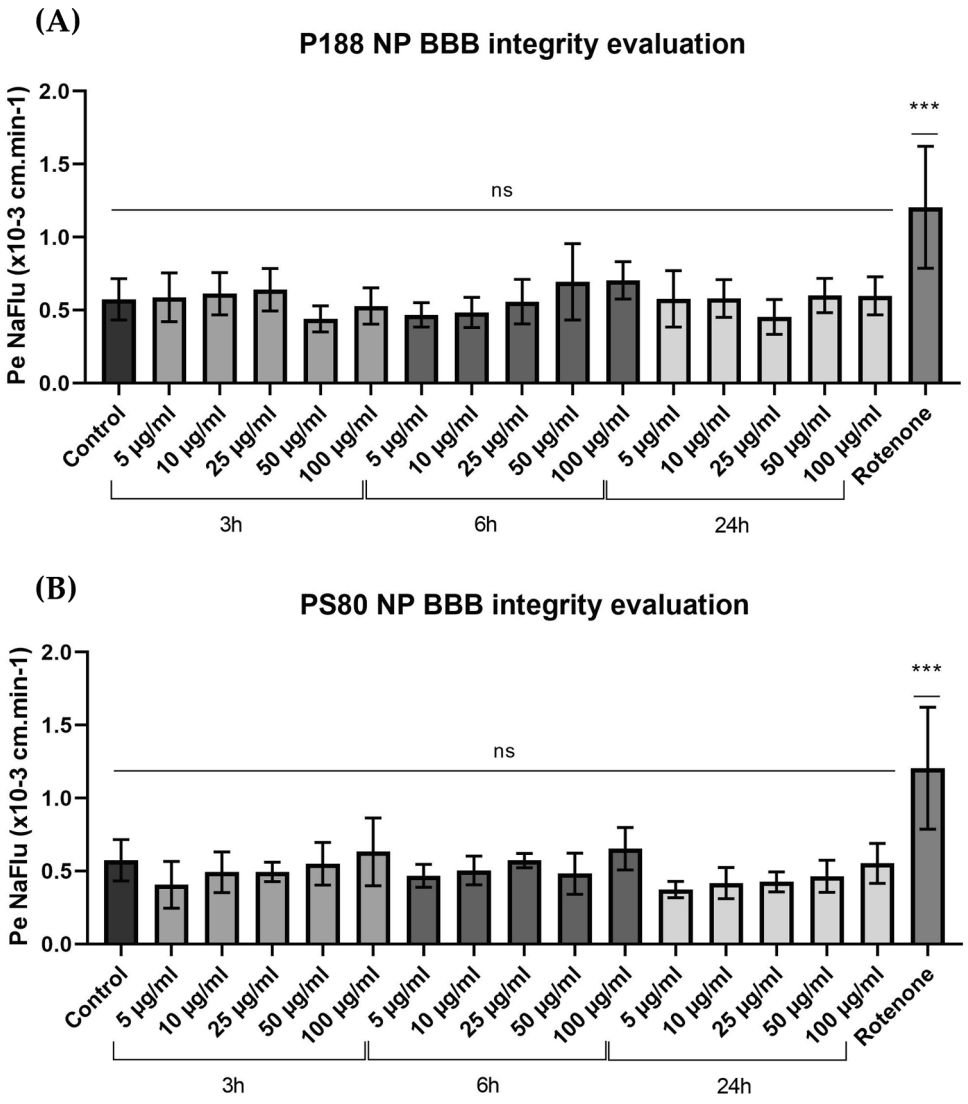

Fig. 3. Endothelial cell permeability coefficient (Pe) values of NaFlu after incubation with NPs. **A.** Evaluation of BBB integrity after P188 NP incubation. **B.** Evaluation of BBB integrity after PS80 NP incubation. Ordinary one-way ANOVA, multiple comparison test, versus negative control were performed. Ns = not significant, *p < 0.05. Control and samples n = 5, N = 2 independent experiments; Rotenone (n = 2, N = 2).

stable around 1.5–2%.

The percentage of NPs recovery was assessed. NPs recovery decreased with increasing incubation time (Fig. 8B). For both formulations, <100% recovery was obtained, with a significant decrease (**p = 0.0020, *p = 0.0111 for P188 and ***p = 0.0004, *p = 0.0274 for PS80) for both NPs after 24 h incubation. This NPs loss could be due to a higher uptake of NPs than the amount of NPs able to undergo transcytosis to the brain (abluminal) compartment. Thus, some NPs were still sequestered inside the BLECs, or degraded inside the cells, and thus could not be recovered.

4. Discussion

In this study, the mechanism of uptake and crossing across the human brain like endothelial cells (BLECs) of PLGA nanoparticles coated with polysorbate 80 or poloxamer 188 produced using the MicroJet reactor® technology were studied. The ability of these surfactant coated PLGA NPs to cross the BBB has already been investigated (Gelperina et al., 2010; Tahara et al., 2011) but not in human pre-clinical model and the exact pathway taken by the nanoparticles has not yet been studied. Some studies performed on PBCA NPs have hypothesized that the protein corona forming around nanoparticles coated with polysorbate 80 or poloxamer 188 could be enriched in apolipoproteins, thus allowing them to cross the BBB by receptor-mediated transcytosis (Ambruosi et al., 2006; Kreuter et al., 2002; Petri et al., 2007). To the best of our knowledge, similar studies have not been performed on surfactant coated PLGA nanoparticles. Furthermore, discrepancies have been noticed where some formulations showed superior crossing ability when coated with P188 and others with PS80 (Lombardo et al., 2020), which might suggest that both surfactants do not exactly share the same uptake mechanism.

Based on these, PLGA nanoparticles were developed and produced using an innovative MicroJet reactor® technology. Using this continuous manufacturing technology for nanoprecipitation method allowed the formation of small nanoparticles with acceptable distribution. The production is easy to number-up by placing different reactors in parallel, thus allowing the use of these nanoparticles for industrial pharmaceutical purpose. Hence, the data acquired in this study were on nanoformulations ready to be scaled-up. The formulation was tailored to obtain nanoparticles lower than 100 nm, as it has been reported that small nanoparticles could be endocytosed more easily by the brain endothelial cells and then further diffuse through the brain extracellular space (Gao and Jiang, 2006; Nance et al., 2012). These formulations could therefore be promising delivery systems for the brain, able to be

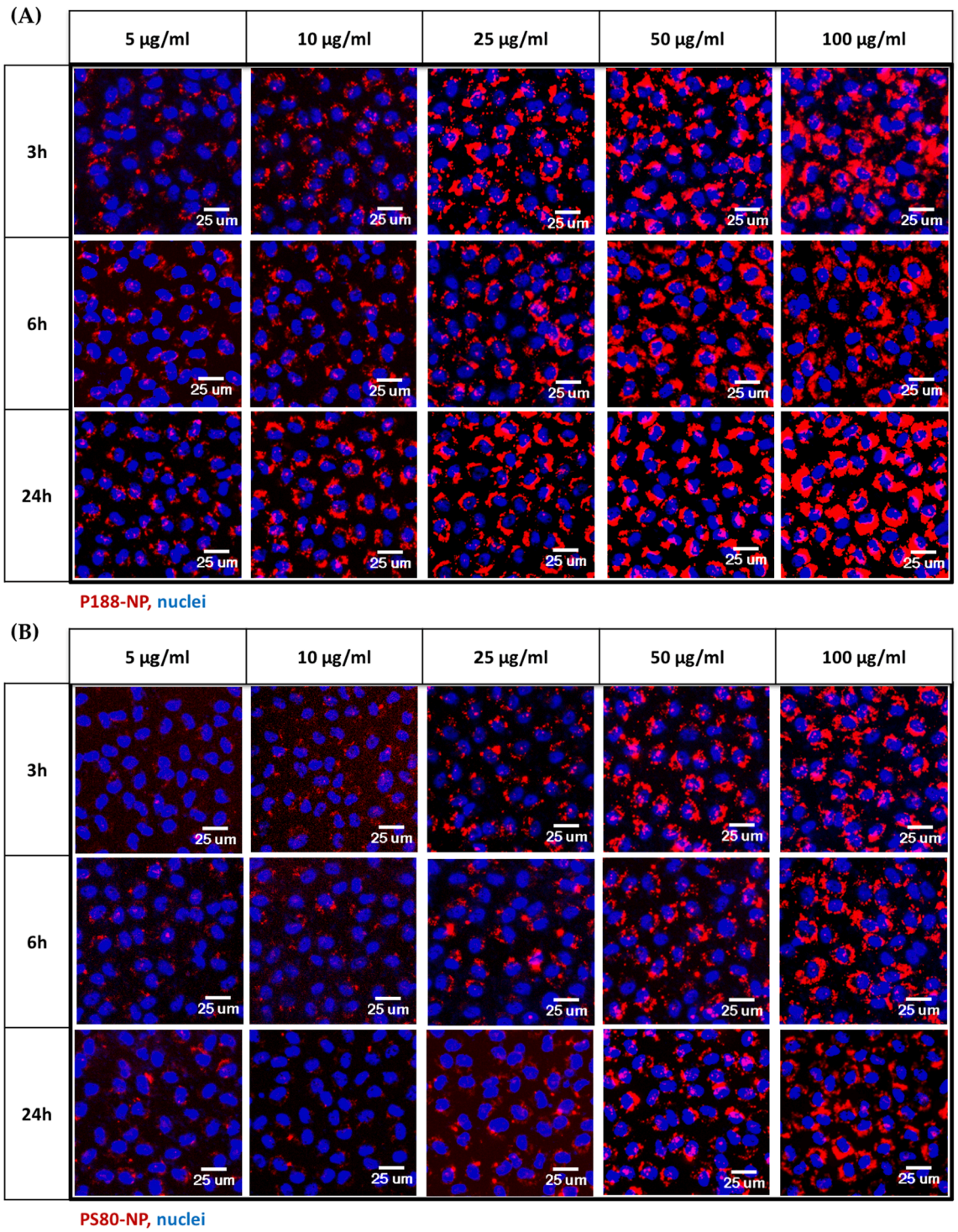

Fig. 4. Confocal images of NPs within the BLECs at different concentrations and incubation times. **A.** BLECs incubated with P188 NP. **B.** BLECs incubated with PS80 NP. Both NPs visualized as red dots, cell nuclei staining in blue. Scale bar = 25 µm. (For interpretation of the references to color in this figure legend, the reader is referred to the web version of this article.)

produced at large scale and to efficiently deliver cargo through the BBB without need of functionalization. Results showed that surfactant coated NPs were produced with a mean size of 76.1 nm for P188 NP and 68.9 nm for PS80 NPs, with an acceptable PDI for industrial purposes (Table 1). The NPs sizes were stable during 10 days in solution. Not-coated PLGA (NC-PLGA) were also developed. However, NC-NPs were not stable after production, as they were produced without any stabilizers or surfactants. Indeed, visible agglomeration was observed one day after production, reinforcing the importance of the use of stabilizers or surfactants not only to enhance the particles functionality to the cells, but also for the proper formulation stability. Thus, these nanoparticles could not be used as good control throughout the experiments, due to their functionalization differences and their instability in cell medium which impacted their cellular interaction abilities.

To study crossing and uptake mechanisms of the surfactant PLGA NPs through the human brain-like endothelial cells (BLECs), patented and well established human BBB in vitro models (Cecchelli et al., 2014; Moya et al., 2021), based on CD34+ stem cells-derived endothelial cells

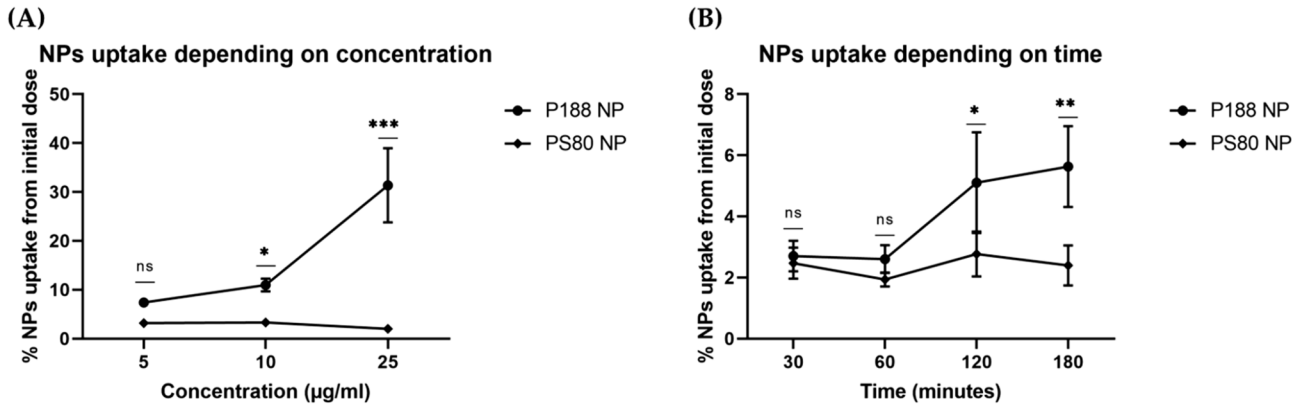

Fig. 5. **A.** NPs uptake within the BLECs depending on NPs concentration after 90 min of incubation. **B.** NPs uptake depending on incubation time, at 10 µg/ml. Samples n = 3 per condition. Statistical analyses performed by two-way ANOVA, multiple comparisons test. Data expressed in mean percentage ± SD. ns = not significant, $p > 0.05$; *$p < 0.05$, **$p < 0.005$.

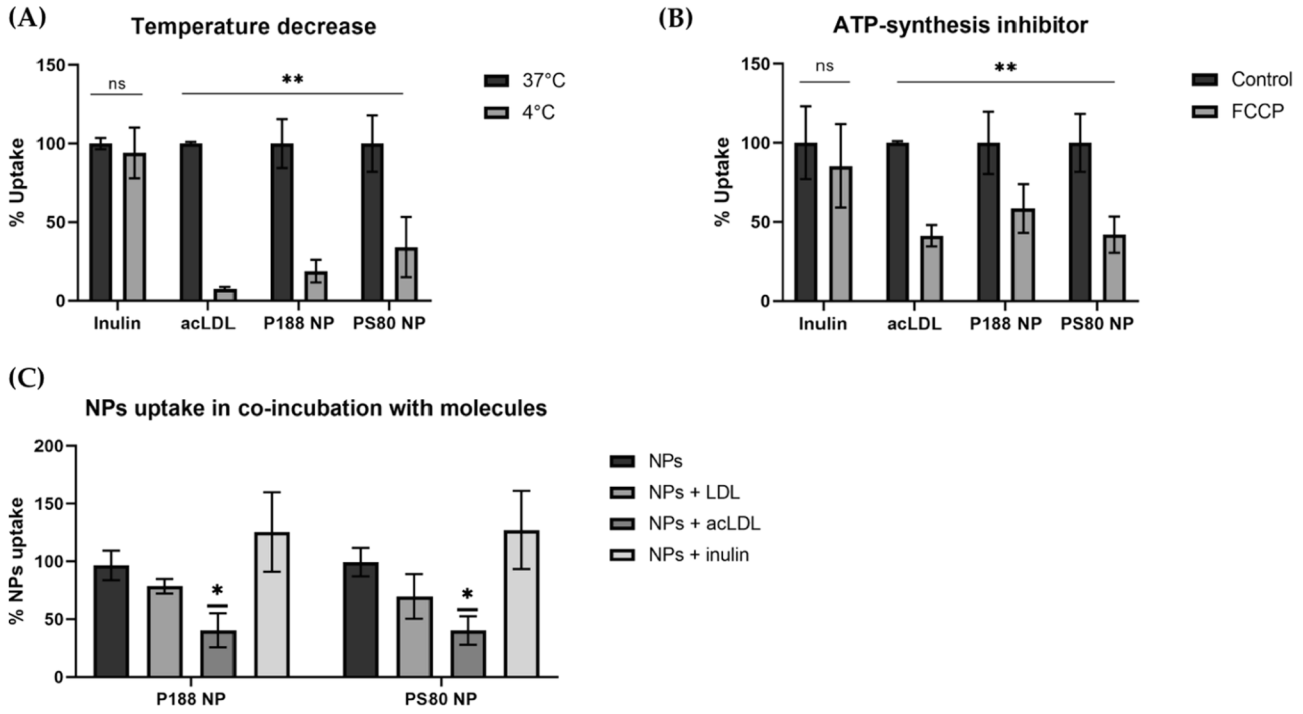

Fig. 6. NPs receptor-mediated active transport. **A.** NPs uptake under temperature decreased conditions. Percentage of inulin, acLDL and NPs uptake after 1 h of incubation at 37 °C and 4 °C. Multiple *t*-test, **$p < 0.005$ and ns = not significant. Inulin and acLDL replicates in n = 3; NPs n = 6, N = 2 independent experiments. **B.** NPs uptake under active transport inhibition. Percentage of NPs uptake after 1 h incubation, with FCCP (ATP inhibitor) pre-incubated 45 min, plus 1 h inulin, acLDL and NPs incubation. Control = molecules/NPs uptake without FCCP. Multiple *t*-test, **$p < 0.005$ and ns = not significant. Inulin and acLDL n = 3; NPs n = 11, N = 4 independent experiments. C. NPs co-incubation with LDL, acLDL, and inulin. Relative percentage of NPs uptake in co-incubation with the molecules, compared to control (NPs only), after incubation 1 h in ECM(5 %HS). Multiple *t*-test, *$p < 0.05$, n = 4; N = 2 independent experiments.

(CD34+-ECs) cocultivated with brain pericytes (Vandenhaute et al., 2011; Shimizu et al., 2011) were used. The use of in vitro BBB models has proven to be useful to evaluate the impact of drugs/compounds toxicity, BBB permeation rates and molecular transport mechanisms within the brain cells in academic research and early-stage drug discovery. In addition, because of the interspecies differences, the use of human pre-clinical in vitro models can be a complement to the in vivo analysis. This model shows a good prediction of the brain delivery of molecules when compared with data obtained in patients (Cecchelli et al., 2014; Moya et al., 2021). In addition, for this NPs interaction study with the BLECs, the fetal calf serum used as a supplement in the cell medium was replaced by human serum 24 h before performing NPs assays (Fig. 2A), since it has been shown that NPs interact not only with the cells but also with components present in the media, like the serum proteins. Indeed, proteins present in biological media can adsorb on the nanoparticle surface to form the so-called protein corona (del Pino et al., 2014). This corona is believed to have a huge effect on the biodistribution of nanoparticles by impacting the cell recognition of the formulation (Monopoli et al., 2012; Capjak et al., 2017). Hence, to obtain results that could be more easily translated to human blood in vivo, the fetal calf serum (FCS) classically used in the cell medium was substituted 24 h before experiments with human serum (HS), to work with a nanoparticle protein corona profile closer to the one expected from in human blood. Then, after 6 days of coculture, the tightly packed cell network of the CD34+-ECs BBB phenotype was validated with the presence of zonula occludens-1 (ZO-1) expression, a protein involved in

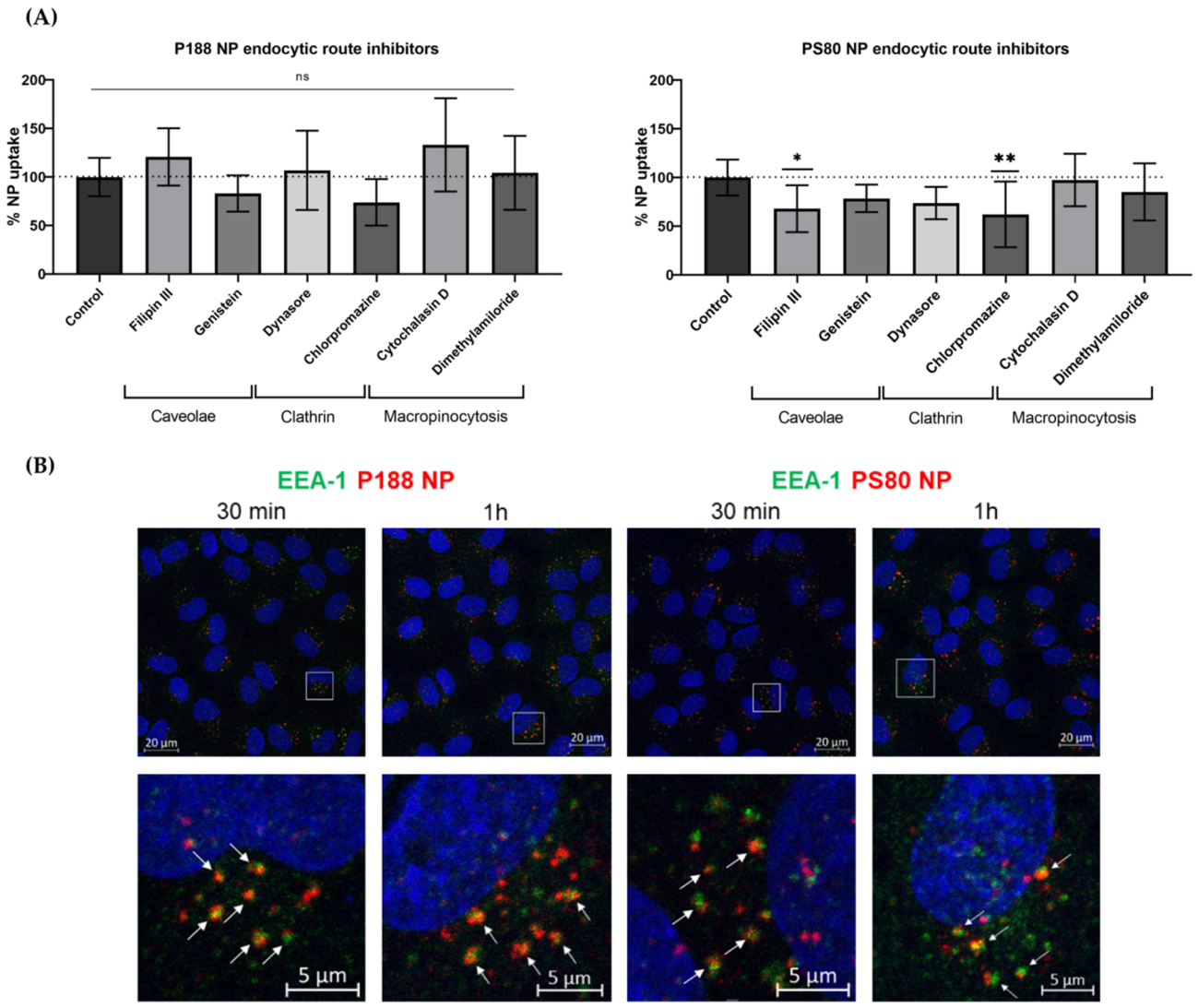

Fig. 7. Endocytosis routes. **A.** Endocytosis routes inhibitors. Percentage of P188 NP and PS80 NP uptake, when a set of caveolae, clathrin and macropinocytosis pathway inhibitors were present in the cell media, after 1-hour incubation. Statistical analyses of one-way ANOVA (multiple comparisons), *$p < 0.05$; ns = not significant. n = 11 replicates; N = 4 independent experiments. **B.** NPs colocalization with early endosome vesicles. Nuclei stained in blue with DAPI, P188 and PS80 NP red fluorescent dots, with EEA-1 vesicles stained green. Initial images scale bar = 20 µm, zoom images scale bar = 5 µm. (For interpretation of the references to color in this figure legend, the reader is referred to the web version of this article.)

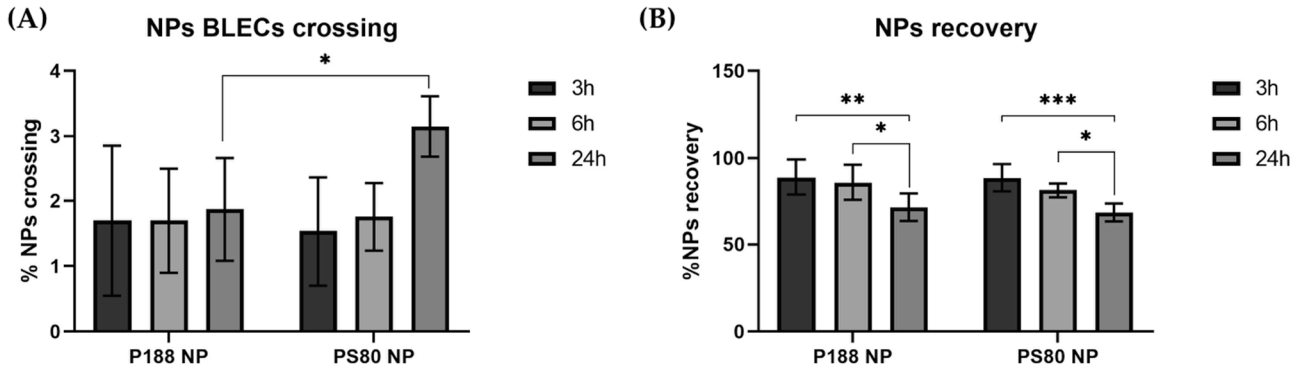

Fig. 8. **A.** Percentage of NP crossing across the human BLECs. P188 NP and PS80 NP were incubated during 3, 6 and 24 h at concentrations 10 µg/ml. **B.** Percentage of NPs recovery at different NPs incubation time. Statistical analyses performed by two-way ANOVA, following Sidaks multiple comparisons test, *$p < 0.05$, **$p < 0.005$, ***$p < 0.0005$. Samples n = 6, in N = 2 independent experiments.

the tight junctions and located continuously at the edge of these cells, in addition with the low paracellular permeability of the model integrity marker NaFlu. No changes were found after substituting the serum (Fig. 2B). Hence, HS replacement 24 h before the experiment did not impact the BBB models integrity.

The surfactant coated PLGA nanoparticles demonstrated good biocompatibility with the BBB model, as no BBB integrity disruption could be observed at a maximum concentration of 100 μg/ml up to 24 h of incubation time (Fig. 3). As hypothesized, both formulations were uptaken and released by the BLECs (Figs. 4, 5 and 8). However, PS80 and P188 NP showed different uptake profiles (Figs. 4 and 5). Indeed, PS80 NP presented a lower uptake than P188 NP. PS80 NP uptake mechanism seemed to reach a maximum at lower concentration and earlier time points, compared to P188 NP.

Next, the uptake mechanism of the nanoparticles was investigated, through colocalization, competition, and inhibition studies. NPs uptakes were temperature and ATP-dependent (Fig. 6A and B) and showed significant competition with acLDL. The uptake was also sensitive to the presence of LDL (Fig. 6C). Thus, results suggested that NPs might be uptaken by endocytosis, through similar receptors as taken by acLDL, which have been reported to be uptaken by scavenger receptors, following the clathrin receptor-mediated endocytosis pathway, and probably with LDLR too, following the caveolae receptor-mediated endocytosis route (Dehouck et al., 1997; Zhu et al., 2011; Kanai et al., 2014; Fukasawa et al., 1996). Moreover, the results obtained with the inhibitor studies showed a significant decrease of PS80 NP uptake when using clathrin and caveolae-dependent pathways inhibitors, as well as a slight but not significant decrease of P188 NP uptake (Fig. 7A). The low effect of the inhibitors on P188 NPs could however be explained by the high uptake of this formulation. As the inhibitors are tested independently, the inhibition of one route did not inhibit the others, which might then hide the significant decrease in NPs uptake through a single inhibited route. Thus, the nanoparticles might be uptaken by the cells through multiple pathways, as also observed with the BBB uptake of silica nanoparticles and glycopeptide PLGA nanoparticles (Georgieva et al., 2011; Tosi et al., 2011). In addition, the presence of serum in the cell medium has been reported to hinder the effect of inhibitors (Francia et al., 2019). However, performing these experiments without serum was not possible as it would have modified the protein corona forming around the nanoparticles. The modification of the protein corona might then have an impact on their internalization pathways and thus lead to results impossible to translate in vivo.

Furthermore, following the cellular metabolic process, after the internalization by endocytosis, both formulations were colocalized with early endosomes (Fig. 7B) (Haqqani et al., 2018; Villaseñor et al., 2019). Moreover, the two formulations were able to be released by the BLECs towards the brain compartment. Similar crossing profiles and percentages were observed between the two formulations at 3 and 6 h (Fig. 8), reaching a significantly higher crossing percentage for PS80 NP after 24 h incubation. Thus, even though P188 NPs were uptaken in higher quantities than PS80 NP, most of them were not able to cross the cell layer. Indeed, it is likely that only a fraction of the uptaken nanoparticles was able to be transcytosed through the BLECs to reach the abluminal compartment, while the remaining NPs might be meant to be degraded. In addition, the low percentage of crossing observed could suggest that the concentration studied of 10 μg/ml was already too high, saturating the crossing mechanism pathway. However, lower concentrations could not be studied as they would have required working under the detection limit of the NPs fluorescence.

Hence, both P188 and PS80 NP produced using the MicroJet reactor technology could be interesting formulations for the delivery of cargo through the BBB to the brain. Further deeper studies could be dedicated to the NPs corona formation within the human blood serum.

5. Conclusion

Hence, in this study, the interaction of the PLGA nanoparticles coated with PS80 or P188, produced using the MicroJet reactor® technology, with human brain like endothelial cells (BLECs) have been analyzed using a well-established in vitro coculture human BBB models supplemented with human serum, specially used for this research approach. Both surfactants coated PLGA NPs presented a good biocompatibility with the BLECs at a maximum concentration tested of 100 μg/ml. Both formulations were internalized in the BLECs, showing different uptake profiles: P188 NP presented a higher and faster uptake by the BLECs than PS80 NP. Moreover, the NPs seemed to be uptaken by the cells through receptor-mediated endocytosis, by presenting a significant competition with acLDL, and a slight competition with LDL, suggesting a possible interaction with the same receptors. The NPs might then be internalized using clathrin and caveolae endocytic routes, being localized afterwards in the early endosome vesicles following the cell trafficking. Both nanoformulations were released afterwards by the BLECs in the same range of percentage despite the significantly higher and faster uptake found for P188 NP in comparison with PS80 NP. Nevertheless, PS80 NP achieved the highest release percentage in 24 h incubation.

Institutional Review Board Statement

The protocol of the collection and use of CD34+-stem cells derived from cord blood was approved by the French Ministry of Higher Education and Research (reference: CODECOH DC2011-1321), and the sample collection was obtained under the written and informed consent from the donor's parent of umbilical cord blood, in accordance with the French Legislation. These cells were harvested thanks to an agreement established between the hospital of Béthune and University of Artois. Moreover, human serum was donated to "l'Etablissement Français du Sang" (EFS) and purchased by Artois University following an agreement signed by the two entities.

Disclosure

E.V and N.M are employees of HCS Pharma; S.L., N.GT and A.T are employees of MyBiotech. S.L developed PLGA NPs and participated in the manuscript writing; N.GT designed the study and supervised the manuscript writing, A.T, E.V and N.M supervised the manuscript writing. The companies legal entities had no role in the design of the study; in the collection, analyses, or interpretation of data; in the writing of the manuscript, or in the decision to publish the results. The other authors declare no conflicts of interest.

Ethics Statements

Authors declare that all the investigation/experiments herein described were carried out following the rules of the Declaration of Helsinki of 1975, revised in 2013 (https://www.wma.net/what-we-do/medical-ethics/declaration-of-helsinki/). Accessed on 22/06/2021.

Declaration of Competing Interest

The authors declare that they have no known competing financial interests or personal relationships that could have appeared to influence the work reported in this paper.

Acknowledgments

Authors would like to warmly thank Gregory Maubon and Marijas Jurisic for the technical supervision of the confocal microscopy, Lucie Dehouck for the Original 12 TW model cell culture training and, Emmanuel Sevin for the training in permeability studies.

Funding

This research project is part of the NANOSTEM project, a Marie Skłodowska-Curie Innovative Training Network (ITN) project which has received funding from the European Union's Horizon 2020 research and

innovation programme under grant agreement N° 764958.

References

Abbott, N.J., Patabendige, A.A.K., Dolman, D.E.M., Yusof, S.R., Begley, D.J., 2010. Structure and function of the blood-brain barrier. Neurobiol. Disease 37, 13–25. https://doi.org/10.1016/j.nbd.2009.07.030.

Hawkins, B.T., Davis, T.P., 2005. The blood-brain barrier/neurovascular unit in health and disease. Pharmacol. Rev. 57, 173–185. https://doi.org/10.1124/pr.57.2.4.

World Health Organization. The Top 10 Causes of Death. <https://www.who.int/news-room/fact-sheets/detail/the-top-10-causes-of-death> (accessed on 5 January 2021).

Abbott, N.J., Rönnbäck, L., Hansson, E., 2006. Astrocyte-endothelial interactions at the blood-brain barrier. Nat. Rev. Neurosci. 7, 41–53. https://doi.org/10.1038/nrn1824.

Lombardo, S.M., Schneider, M., Türeli, A.E., Türeli, N.G., 2020. Key for crossing the BBB with nanoparticles: the rational design. Beilstein. J. Nanotechnol. 11, 866–883. https://doi.org/10.3762/bjnano.11.72.

Ambruosi, A., Gelperina, S., Khalansky, A., Tanski, S., Theisen, A., Kreuter, J., 2006. Influence of surfactants, polymer and doxorubicin loading on the anti-tumour effect of poly(butyl cyanoacrylate) nanoparticles in a rat glioma model. J. Microencapsul. 23, 582–592. https://doi.org/10.1080/02652040600788080.

Ren, T., Xu, N., Cao, C., Yuan, W., Yu, X., Chen, J., Ren, J., 2009. Preparation and therapeutic efficacy of polysorbate-80-coated amphotericin B/PLA-b-PEG nanoparticles. J. Biomater. Sci. Polym. Ed. 20, 1369–1380. https://doi.org/10.1163/092050609X12457418779185.

Gelperina, S., Maksimenko, O., Khalansky, A., Vanchugova, L., Shipulo, E., Abbasova, K., Berdiev, R., Wohlfart, S., Chepurnova, N., Kreuter, J., 2010. Drug delivery to the brain using surfactant-coated poly(lactide-co-glycolide) nanoparticles: influence of the formulation parameters. Euro. J. Pharmaceut. Biopharmaceut. 74, 157–163. https://doi.org/10.1016/j.ejpb.2009.09.003.

Kreuter, J., Shamenkov, D., Petrov, V., Ramge, P., Cychutek, K., Koch-Brandt, C., Alyautdin, R., 2002. Apolipoprotein-mediated transport of nanoparticle-bound drugs across the blood-brain barrier. J. Drug Target. 10, 317–325. https://doi.org/10.1080/10611860290031877.

Petri, B., Bootz, A., Khalansky, A., Hekmatara, T., Müller, R., Uhl, R., Kreuter, J., Gelperina, S., 2007. Chemotherapy of brain tumour using doxorubicin bound to surfactant-coated poly(butyl cyanoacrylate) nanoparticles: revisiting the role of surfactants. J. Control. Release 117, 51–58. https://doi.org/10.1016/j.jconrel.2006.10.015.

Tahara, K., Miyazaki, Y., Kawashima, Y., Kreuter, J., Yamamoto, H., 2011. Brain targeting with surface-modified poly(d, l-Lactic-Co-Glycolic Acid) nanoparticles delivered via carotid artery administration. Euro. J. Pharmaceut. Biopharmaceut. 77, 84–88. https://doi.org/10.1016/j.ejpb.2010.11.002.

Chaturvedi, M., Molino, Y., Sreedhar, B., Khrestchatisky, M., Kaczmarek, L., 2014. Tissue inhibitor of matrix metalloproteinases-1 loaded poly(lactic-co-glycolic acid) nanoparticles for delivery across the blood-brain barrier. Int. J. Nanomed. 9, 575–588. https://doi.org/10.2147/IJN.S54750.

Miyazawa, T., Nakagawa, K., Harigae, T., Onuma, R., Kimura, F., Fujii, T., Miyazawa, T., 2015. Distribution of β-carotene-encapsulated polysorbate 80-coated poly(D, L-Lactide-Co-Glycolide) nanoparticles in rodent tissues following intravenous administration. Int. J. Nanomed. 10, 7223–7230. https://doi.org/10.2147/IJN.S94336.

U.S Food and Drug Administration Inactive Ingredient Search for Approved Drug Products. <https://www.accessdata.fda.gov/scripts/cder/iig/index.cfm> (accessed on 5 April 2022).

Makadia, H.K., Siegel, S.J., 2011. Poly Lactic-Co-Glycolic Acid (PLGA) as Biodegradable Controlled Drug Delivery Carrier. Polymers (Basel) 3, 1377–1397. https://doi.org/10.3390/polym3031377.

Lee, B.K., Yun, Y., Park, K., 2016. PLA micro- and nano-particles. Adv. Drug Deliv. Rev. 107, 176–191. https://doi.org/10.1016/j.addr.2016.05.020.

Schiller, S., Hanefeld, A., Schneider, M., Lehr, C.-M., 2020. Towards a continuous manufacturing process of protein-loaded polymeric nanoparticle powders. AAPS PharmSciTech. 21, 269. https://doi.org/10.1208/s12249-020-01814-w.

Schiller, S., Hanefeld, A., Schneider, M., Lehr, C.-M., 2015. Focused ultrasound as a scalable and contact-free method to manufacture protein-loaded PLGA nanoparticles. Pharm. Res. 32, 2995–3006. https://doi.org/10.1007/s11095-015-1681-7.

Valencia, P.M., Farokhzad, O.C., Karnik, R., Langer, R., 2012. Microfluidic technologies for accelerating the clinical translation of nanoparticles. Nat. Nanotechnol. 7, 623–629. https://doi.org/10.1038/nnano.2012.168.

Makgwane, P.R., Ray, S.S., 2014. Synthesis of nanomaterials by continuous-flow microfluidics: a review. J. Nanosci. Nanotechnol. 14, 1338–1363. https://doi.org/10.1166/jnn.2014.9129.

Günday Türeli, N., Türeli, A.E., Schneider, M., 2016. Optimization of ciprofloxacin complex loaded PLGA nanoparticles for pulmonary treatment of cystic fibrosis infections: design of experiments approach. Int. J. Pharmaceut. 515, 343–351. https://doi.org/10.1016/j.ijpharm.2016.10.025.

Cecchelli, R., Aday, S., Sevin, E., Almeida, C., Culot, M., Dehouck, L., Coisne, C., Engelhardt, B., Dehouck, M.-P., Ferreira, L., Klein, R., 2014. A stable and reproducible human blood-brain barrier model derived from hematopoietic stem cells. PLoS One 9 (6), e99733.

Moya, E.L.J., Vandenhaute, E., Rizzi, E., Boucau, M.-C., Hachani, J., Maubon, N., Gosselet, F., Dehouck, M.-P., 2021. Miniaturization and automation of a human in vitro blood-brain barrier model for the high-throughput screening of compounds in the early stage of drug discovery. Pharmaceutics 13, 892.

Pedroso, D.C.S., Tellechea, A., Moura, L., Fidalgo-Carvalho, I., Duarte, J., Carvalho, E., Ferreira, L., Gelain, F., 2011. Improved survival, vascular differentiation and wound healing potential of stem cells co-cultured with endothelial cells. PLOS ONE 6 (1), e16114.

Vandenhaute, E., Dehouck, L., Boucau, M.-C., Sevin, E., Uzbekov, R., Tardivel, M., Gosselet, F., Fenart, L., Cecchelli, R., Dehouck, M.-P., 2011. Modelling the neurovascular unit and the blood-brain barrier with the unique function of pericytes. CNR 8, 258–269. https://doi.org/10.2174/156720211798121016.

Shimizu, F., Sano, Y., Abe, M., Maeda, T., Ohtsuki, S., Terasaki, T., Kanda, T., 2011. Peripheral nerve pericytes modify the blood-nerve barrier function and tight junctional molecules through the secretion of various soluble factors. J. Cell. Physiol. 226, 255–266. https://doi.org/10.1002/jcp.22337.

Vandenhaute, E., Drolez, A., Sevin, E., Gosselet, F., Mysiorek, C., Dehouck, M.-P., 2016. Adapting coculture in vitro models of the blood-brain barrier for use in cancer research: maintaining an appropriate endothelial monolayer for the assessment of transendothelial migration. Lab. Invest. 96, 588–598. https://doi.org/10.1038/labinvest.2016.35.

Ravenstijn, P.G.M., Merlini, M., Hameetman, M., Murray, T.K., Ward, M.A., Lewis, H., Ball, G., Mottart, C., de Ville de Goyet, C., Lemarchand, T., van Belle, K., O'Neill, M. J., Danhof, M., de Lange, E.C.M., 2008. The exploration of rotenone as a toxin for inducing parkinson's disease in rats, for application in BBB transport and PK-PD experiments. J. Pharmacol. Toxicol. Meth. 57 (2), 114–130.

Dehouck, B., Fenart, L., Dehouck, M.-P., Pierce, A., Torpier, G., Cecchelli, R., 1997. A new function for the LDL receptor: transcytosis of LDL across the blood-brain barrier. J. Cell Biol. 138, 877–889. https://doi.org/10.1083/jcb.138.4.877.

Candela, P., Gosselet, F., Saint-Pol, J., Sevin, E., Boucau, M.-C., Boulanger, E., Cecchelli, R., Fenart, L., 2010. Apical-to-basolateral transport of amyloid-β peptides through blood-brain barrier cells is mediated by the receptor for advanced glycation end-products and is restricted by P-glycoprotein. J. Alzheimer's Disease 22, 849–859. https://doi.org/10.3233/JAD-2010-100462.

Saint-Pol, J., Candela, P., Boucau, M.-C., Fenart, L., Gosselet, F., 2013. Oxysterols decrease apical-to-basolateral transport of Aß peptides via an ABCB1-mediated process in an in vitro blood-brain barrier model constituted of bovine brain capillary endothelial cells. Brain Res. 1517, 1–15. https://doi.org/10.1016/j.brainres.2013.04.008.

Okura, T., Hattori, A., Takano, Y., Sato, T., Hammarlund-Udenaes, M., Terasaki, T., Deguchi, Y., 2008. Involvement of the pyrilamine transporter, a putative organic cation transporter, in blood-brain barrier transport of oxycodone. Drug Metab. Dispos. 36, 2005–2013. https://doi.org/10.1124/dmd.108.022087.

Georgieva, J.V., Kalicharan, D., Couraud, P.-O., Romero, I.A., Weksler, B., Hoekstra, D., Zuhorn, I.S., 2011. Surface characteristics of nanoparticles determine their intracellular fate in and processing by human blood-brain barrier endothelial cells in vitro. Mol. Therapy 19, 318–325. https://doi.org/10.1038/mt.2010.236.

Morad, G., Carman, C.V., Hagedorn, E.J., Perlin, J.R., Zon, L.I., Mustafaoglu, N., Park, T.-E., Ingber, D.E., Daisy, C.C., Moses, M.A., 2019. Tumor-derived extracellular vesicles breach the intact blood-brain barrier via transcytosis. ACS Nano 13, 13853–13865. https://doi.org/10.1021/acsnano.9b04397.

Gao, K., Jiang, X., 2006. Influence of particle size on transport of methotrexate across blood brain barrier by polysorbate 80-coated polybutylcyanoacrylate nanoparticles. Int. J. Pharmaceut. 310, 213–219. https://doi.org/10.1016/j.ijpharm.2005.11.040.

Nance, E.A., Woodworth, G.F., Sailor, K.A., Shih, T.-Y., Xu, Q., Swaminathan, G., Xiang, D., Eberhart, C., Hanes, J., 2012. A dense poly(ethylene glycol) coating improves penetration of large polymeric nanoparticles within brain tissue. Sci. Transl. Med. 4, 149ra119. https://doi.org/10.1126/scitranslmed.3003594.

del Pino, P., Pelaz, B., Zhang, Q., Maffre, P., Ulrich Nienhaus, G., Parak, W.J., 2014. Protein corona formation around nanoparticles – from the past to the future. Mater. Horizons 1, 301–313. https://doi.org/10.1039/C3MH00106G.

Monopoli, M.P., Åberg, C., Salvati, A., Dawson, K.A., 2012. Biomolecular coronas provide the biological identity of nanosized materials. Nat. Nanotechnol. 7, 779–786. https://doi.org/10.1038/nnano.2012.207.

Capjak, I., Goreta, S.Š., Jurašin, D.D., Vrček, I.V., 2017. How protein coronas determine the fate of engineered nanoparticles in biological environment. Arh. Hig. Rada Toksikol. 68, 245–253. https://doi.org/10.1515/aiht-2017-68-3054.

Zhu, X.-D., Zhuang, Y., Ben, J.-J., Qian, L.-L., Huang, H.-P., Bai, H., Sha, J.-H., He, Z.-G., Chen, Q., 2011. Caveolae-dependent endocytosis is required for class a macrophage scavenger receptor-mediated apoptosis in macrophages*. J. Biol. Chem. 286, 8231–8239. https://doi.org/10.1074/jbc.M110.145888.

Kanai, Y., Wang, D., Hirokawa, N., 2014. KIF13B enhances the endocytosis of LRP1 by recruiting LRP1 to Caveolae. J. Cell Biol. 204, 395–408. https://doi.org/10.1083/jcb.201309066.

Fukasawa, M., Adachi, H., Hirota, K., Tsujimoto, M., Arai, H., Inoue, K., 1996. SRB1, a class B scavenger receptor, recognizes both negatively charged liposomes and apoptotic cells. Exp. Cell Res. 222, 246–250. https://doi.org/10.1006/excr.1996.0030.

Tosi, G., Fano, R.A., Bondioli, L., Badiali, L., Benassi, R., Rivasi, F., Ruozi, B., Forni, F., Vandelli, M.A., 2011. Investigation on mechanisms of glycopeptide nanoparticles for drug delivery across the blood-brain barrier. Nanomedicine 6, 423–436. https://doi.org/10.2217/nnm.11.11.

Francia, V., Yang, K., Deville, S., Reker-Smit, C., Nelissen, I., Salvati, A., 2019. Corona composition can affect the mechanisms cells use to internalize nanoparticles. ACS Nano 13, 11107–11121. https://doi.org/10.1021/acsnano.9b03824.

Haqqani, A.S., Delaney, C.E., Brunette, E., Baumann, E., Farrington, G.K., Sisk, W., Eldredge, J., Ding, W., Tremblay, T.-L., Stanimirovic, D.B., 2018. endosomal trafficking regulates receptor-mediated transcytosis of antibodies across the blood brain barrier. J. Cereb. Blood Flow Metab. 38, 727–740. https://doi.org/10.1177/0271678X17740031.

Villaseñor, R., Lampe, J., Schwaninger, M., Collin, L., 2019. Intracellular transport and regulation of transcytosis across the blood-brain barrier. Cell. Mol. Life Sci. 76, 1081–1092. https://doi.org/10.1007/s00018-018-2982-x.